Electronic Supplementary Material (ESI) for Materials Horizons.
This journal is © The Royal Society of Chemistry 2019

Electronic supplementary information

Generalized Way to Make Temperature Tunable Conductor-Insulator Transition Liquid Metal Composites in Diverse Range

Sen Chen [#a, c, d], Hong-Zhang Wang [#b], Xu-Yang Sun [b], Qian Wang [a,d], Xiang-Jiang Wang [b], Liu-Biao Chen [c, d], Lun-Jia Zhang [a, c, d], Rui Guo [b], Jing Liu [* a, b, c,d]

[a]*Beijing Key Laboratory of Cryo-Biomedical Engineering, Technical Institute of Physics and Chemistry, Chinese Academy of Sciences, Beijing 100190, China.*

[b]*Department of Biomedical Engineering, School of Medicine, Tsinghua University, Beijing 100084, China.*

[c]*School of Future Technology, University of Chinese Academy of Sciences, Beijing 100049, China.*

[d]*Chinese Academy of Sciences Key Laboratory of Cryogenics, Technical Institute of Physics and Chemistry, Beijing 100190, China.*

# These two authors contributed equally to this research.

† Electronic Supplementary Information (ESI) available: Details on the experimental procedures, and supplementary Movies S1-S3 and Figures S1-S8.

* *E-mail: jliu@mail.ipc.ac.cn*

Experimental Section

Preparation of LCIT materials. Liquid metal mentioned here are composed of 75.5% gallium (Nanjing Jinmei Gallium LTD., 99.999%) and 24.5% indium (Shaoguan Jinyuan Industrial Co., Ltd., 99.999%) by weight, heating and mixing via magnetic stirrer for 20 minutes. The LCIT materials are composed of liquid metal droplets and dimethicone. The specific preparation method is as follows. The liquid metal and the dimethicone are mixed together by a mechanical stirrer for a stirring time of 20 s and a speed of 600 rpm.

Acquisition of micrograph of the LCIT materials. The images in Figure 2a were acquired with environmental scanning electron microscope (ESEM; QUANTA FEG 250, America). Microstructure photos of LCIT materials on Figure S1 were obtained from the Metallographic microscope and SEM (Quata 200).

Thermal characterization. The phase change point was measured by differential scanning calorimetry (NETZSCH DSC200F3, Germany). Besides, the imaging data and the infrared images of the LCIT materials were recorded by the Sony Digital Video (FDR-AX40) and the far-infrared thermograph imaging system (FLIR SC620, FLIR Systems Inc, USA), respectively.

Electrical properties testing: The resistivity of LCIT materials in different temperature was measured by Physical Property Measurement System (PPMS). Current-Voltage curves of LCIT were measured directly with Agilent. Multimeter was also applied to detect the resistance.

Wettability test : The experiment of the wettability between the liquid metal and the dimethicone was taken by the contact angle instrument (POWEREACH JC2000D3, China).

Table S1. Liquid density and solid density of metals and theirs volume expansion ratio during liquid-solid phase transition.

Metals	Solid phase density (ρ_S, g/cm^3) [1,2]	Liquid phase density (ρ_L, g/cm^3) [1,2]	Volume expansion ratio (Φ, %)
Fe	7.87	6.98	11.31
Cu	8.96	8.02	10.49
Ag	10.05	9.32	7.26
Al	2.7	2.37	12.22
Mg	1.73	1.58	08.67
Ti	4.54	4.11	9.47
Li	0.53	0.51	3.77
Hg	14.19	13.55	4.51
Zn	7.13	6.57	7.85
Sn	7.31	6.99	4.38
In	7.31	7.02	3.97
Ga	5.9	6.08	-3.05
Bi	9.75	10.05	-3.08
Cr	7.19	6.3	12.38
Cs	1.873	1.84	1.76
K	0.862	0.83	3.71
Mn	7.21	5.95	17.47
Na	0.971	0.927	4.53
Ni	8.902	7.81	12.27
Pb	11.35	10.66	6.08
Fe	7.87	6.98	11.31
Ca	1.55	1.38	10.97
Pt	21.45	19.77	7.83

Au	19.3	17.31	10.31
Dy	8.551	8.37	2.11
Er	9.066	8.86	2.27
Eu	5.244	5.13	2.17
Cd	8.65	7.4	14.45
Hf	13.31	12	9.84
Ho	8.795	8.34	5.17
Ir	22.42	19	15.25
Co	8.9	7.55	15.17
La	6.145	5.94	3.34
Lu	9.841	9.3	5.50
Be	1.848	1.69	8.55
Mo	10.22	9.33	8.71
Nd	7.008	6.89	1.68
Os	22.57	20	11.39
Pd	12.02	10.38	13.64
Pr	6.773	6.5	4.03
Pu	19.84	16.63	16.17
Rb	1.53	1.46	4.79
Re	21.02	18.9	10.08
Rh	12.41	10.7	13.78
Ru	12.41	10.65	14.18
Sb	6.69	6.53	2.39
Sc	2.989	2.8	6.32
Sm	7.52	7.16	4.79
Sr	2.54	2.37	6.69
Ta	16.654	15	9.93
Tb	8.23	7.65	7.05
Te	6.24	5.7	8.65

Tl	11.85	11.22	5.32
U	18.95	17.3	8.71
V	6.11	5.5	9.98
W	19.3	17.6	8.81
Y	4.469	4.24	5.12
Yb	6.903	6.21	10.04
Zr	6.506	5.8	10.85
Cd	8.65	7.996	7.56
Ce	6.77	6.55	3.25

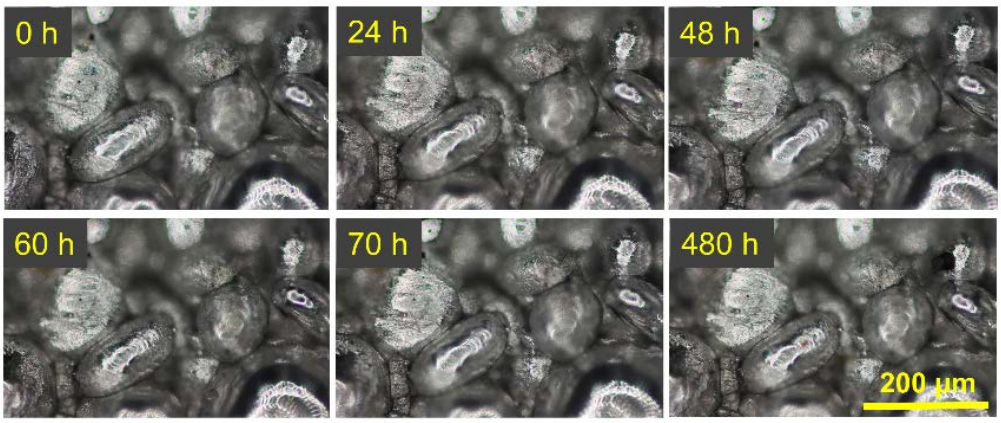

Fig. S1. Within the 480h, the whole structure of the LCIT materials did not change over time, indicating that LCIT materials are stable with time.

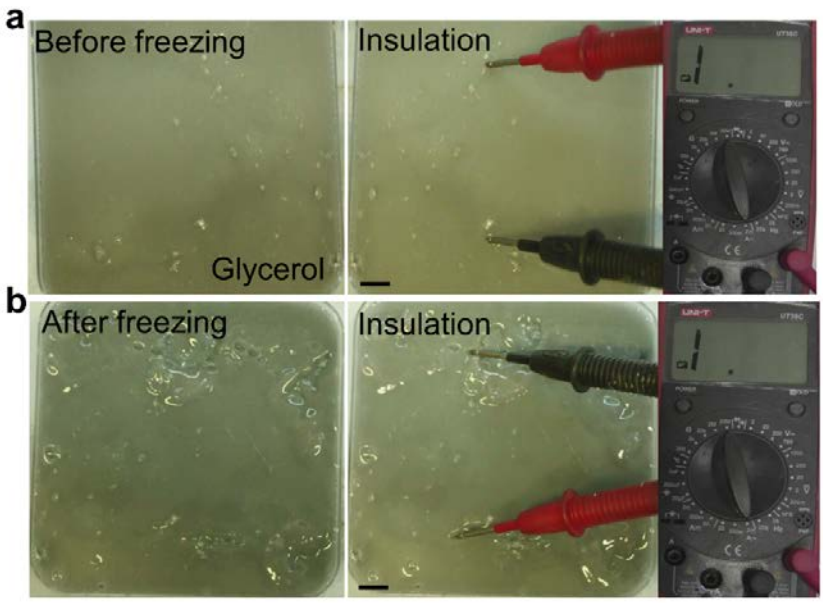

Fig. S2 Example of glycerol as a solvent. a. Liquid metal droplets dispersed in glycerol are non-conductive before freezing. b. Liquid metal droplets dispersed in glycerol are still non-conductive after freezing. Scale bars, 10 mm. Here, the mixed solution will swell upwards and destroy the structure of the entire composite when freezing, thereby leading to the non-conductive after freezing.

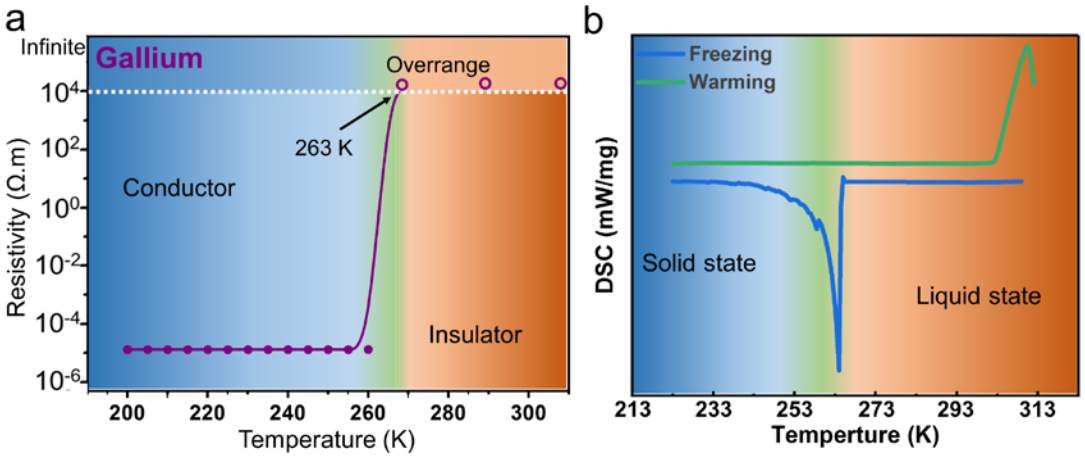

Fig. S3 Resistance transition point and phase transition point of LCIT materials consisting of pure gallium and dimethicone. a. PPMS test shows the resistance transition point of such LCIT materials. Here, these overrange data were presented with symbolic points. b. DSC test shows the phase transition point of such LCIT materials. Here, we can clearly see that the temperature of the phase transition point and the resistance transition point are almost the same and increase to 263K.

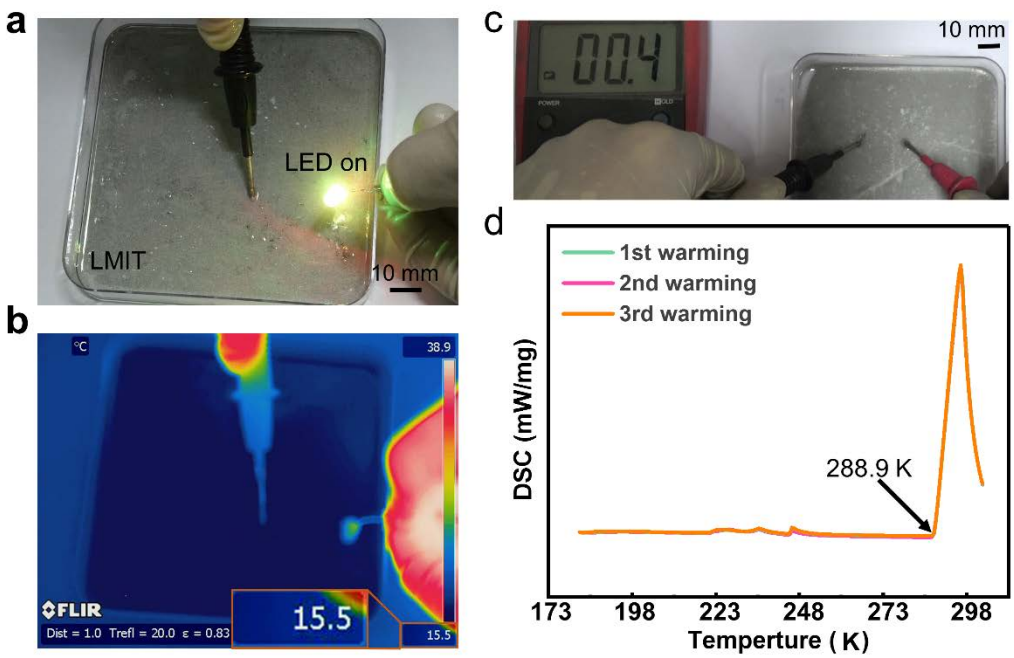

Fig. S4 Ga-based alloys maintain electrical conductivity. a. As the temperature rises, the LED light is still bright, indicating that the LCIT material is in a conductive state. b. The experimental infrared image shows that the LCIT material is still conductive at 288.7K (15.5°C). c. DSC test curve of $GaIn_{24.5}$ shows that the phase change point is 288.9K. Here, the maximum temperature at which LCIT materials can conduct depends on the melting point of liquid metal droplets.

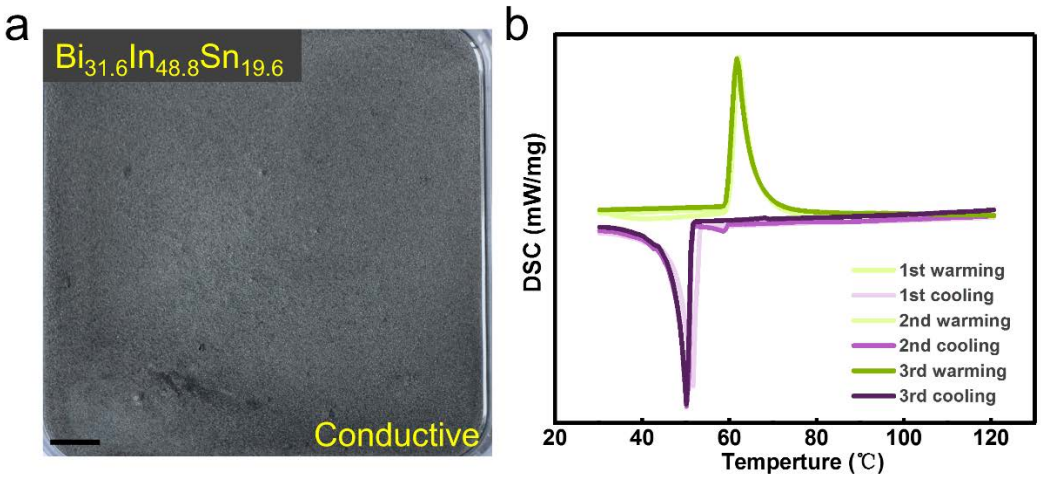

Fig. S5 The experiments about Bi-based alloy ($Bi_{31.6}In_{48.8}Sn_{19.6}$). a. Photograph of Bi-based alloys that can conduct electricity at room temperature. b. DSC test

curve of Bi-based alloys show that the phase change point is above 233K, indicating that Bi-based alloy is in solid state at room temperature, which explains the reason for its conduction at room temperature. Scale bars, 10 mm.

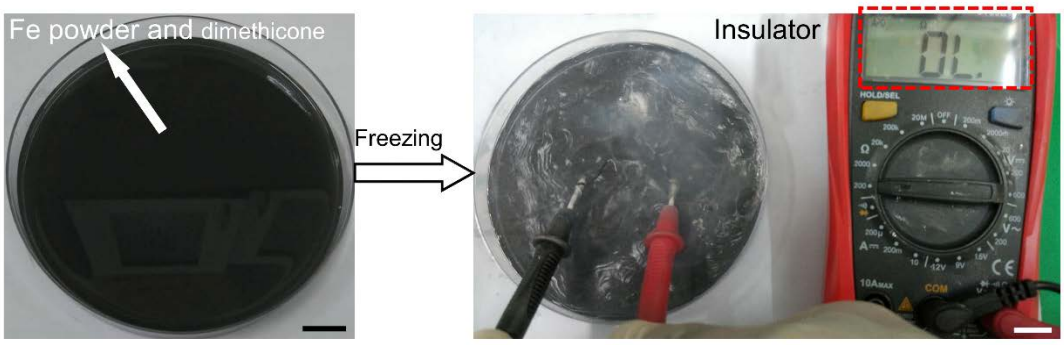

Fig. S6. After freezing, the Fe powder immersed in dimethicone is still not conductive. Scale bars, 10 mm.

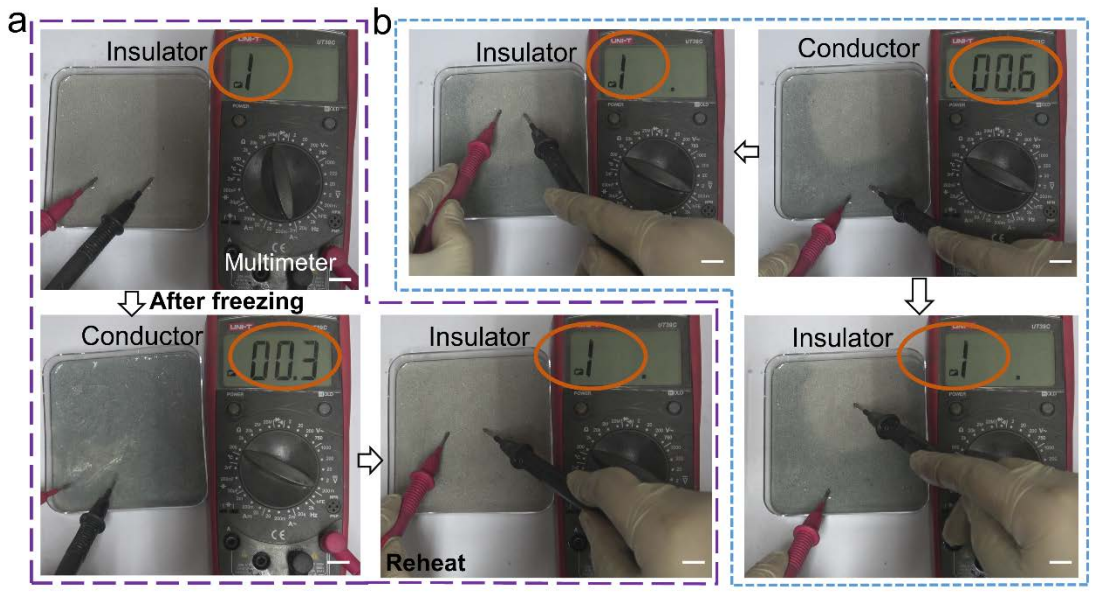

Fig. S7. Visualized circuit composed of LCIT materials. a. As the resistance changes reversibly, the color change is also reversible. b. Different colors correspond to different conductivity for the same sample. Here, the deep color represents excellent electrical conductivity and multimeter is used to test whether the material is conductive. Scale bars, 10 mm.

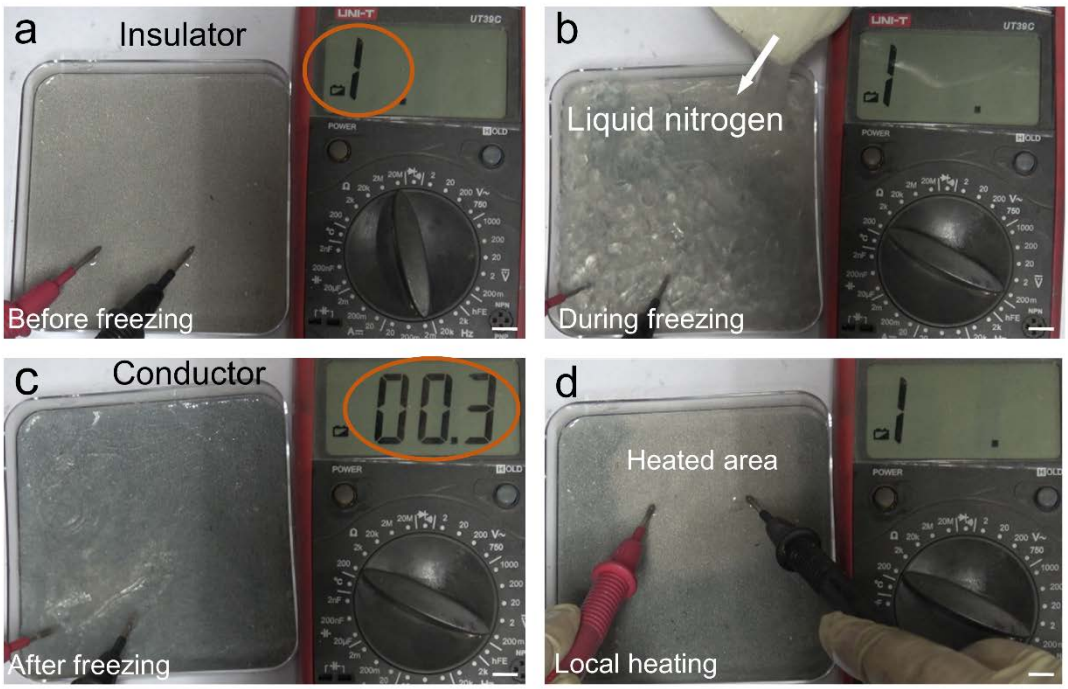

Fig. S8. Performance of LCIT materials at liquid nitrogen temperature. a. The LCIT material is in an insulating state before freezing. b. Pour liquid nitrogen to freeze the LCIT material. c. After freezing with liquid nitrogen, the LCIT material becomes a conductive state. At this time, liquid nitrogen is still present on the surface of the LCIT material. d. After local heating, the heated area with changed color becomes insulating again. The whole process indicates that the LCIT materials still work well at liquid nitrogen temperature. Scale bars, 10 mm.

Movie S1. The LCIT materials become conductive after freezing and recover to be insulating after heating. The liquid appearing in the video is liquid nitrogen. Whether the bulb is on indicates whether the LCIT material is conductive.

Movie S2. Insulated areas can be customized with laser. Here, the area irradiated by the laser becomes insulated.

Movie S3. Self-healing immediately when the LCIT materials suffer severe damage. At this case, the LCIT materials remain liquid.

References

1. D. Lide and etal, *CRC Handbook of chemistry and physics*, CRC Press, 1992.
2. J. A. Dean, *Advanced Manufacturing Processes*, 2010, **5**, 687-688.